Magneto-Coulomb Effect in Carbon Nanotube Quantum Dots Filled with Magnetic Nanoparticles

S. Datta,[1] L. Marty,[1] J. P. Cleuziou,[1] C. Tilmaciu,[2] B. Soula,[2] E. Flahaut,[2] and W. Wernsdorfer[1]
[1]*Institut Néel, CNRS and Université Joseph Fourier, B.P. 166, 25 Avenue des Martyrs, 38042 Grenoble Cedex 9, France*
[2]*Université de Toulouse, UPS, INP, Institut Carnot Cirimat, 118 route de Narbonne, 31062 Toulouse Cedex 9, France*
(Received 8 May 2011; published 27 October 2011)

Electrical transport measurements of carbon nanotubes filled with magnetic iron nanoparticles are reported. Low-temperature (40 mK) magnetoresistance measurements showed conductance hysteresis with sharp jumps at the switching fields of the nanoparticles. Depending on the gate voltage, positive or negative hysteresis was observed. The results are explained in terms of a magneto-Coulomb effect: The spin flip of the iron island at a nonzero magnetic field causes a shift of the chemical potential induced by the change of Zeeman energy; i.e., an effective charge variation is detected by the nanotube quantum dot.

DOI: 10.1103/PhysRevLett.107.186804 PACS numbers: 73.23.−b, 75.60.Jk, 85.65.+h

Manipulating single spins confined or coupled to nanoconductors has become a central issue of molecular spintronics [1–3]. Recent progress in combining the two fields of research, quantum electronics [4] and nanomagnetism [5], has revealed the electric field control of spin-polarized transport, resulting from spin-valve [6] and magneto-Coulomb effects [7]. Ono, Shimada, and Ootuka observed first a magneto-Coulomb effect (MCE) in a single-electron transistor of a metallic island connected to two ferromagnetic leads [7]. This effect was characterized by an enhanced magnetoresistance (MR) of the island in the Coulomb blockade regime, which originated from the Zeeman energy of the ferromagnetic contacts, inducing an opposite shift of the majority and minority spin energy bands. This results in a modification of the island's chemical potential, which is equivalent to an effective electrostatic gating. Thus, the MCE enabled them to tune the single-electron transistor by the magnetic field, leading to magneto-Coulomb oscillations [8], reminiscent of the Coulomb blockade oscillations occurring as a function of gate voltage. Other groups reported a MCE occurring in ferromagnetic semiconductor single-electron transistors [9] and an anisotropic MCE [10], caused by the magnetization rotation of ferromagnetic leads connected to a single Au nanoparticle [11]. Indeed, different MCEs may be relevant in various configurations, in which a device sensitive to Coulomb interactions is coupled to a magnetic material.

Here, we investigate a new kind of MCE, arising in carbon nanotube quantum dots coupled to single encapsulated magnetic nanoparticles. A large controllable MR signal is expected, since the positions of the discrete energy levels of the quantum dot are tuned by a gate voltage [12]. Such a MCE signature is difficult to extract in the conventional spin-valve geometry [13], in which other mechanisms (spin injection [14,15], spin-dependent quantum interference [16], etc.) can play a dominant role. Original molecular spintronics device configurations [2,3] could provide new methods for taking advantage of the MCE in nanostructures: Carbon nanotubes are an ideal one-dimensional conducting system for the local coupling of nanometer-sized magnets (magnetic nanoparticles, single-molecular magnets, etc.) by means of surface functionalization [17] or inner core filling [18,19]. The energy levels of a nanotube quantum dot are expected to be sensitive to any electrostatic change in their close environment and so to the Zeeman energy of the interacting ferromagnet in an applied magnetic field. Such an electrostatic effect would thus allow a single magnetic nanoparticle to be coupled to the charge transport in the quantum dot. In this Letter, we report on this new kind of MCE in carbon nanotube quantum dots filled with magnetic nanoparticles.

The MCE reported here is investigated in quantum transport measurements of double-wall carbon nanotubes (DWCNTs), filled in their inner shell with Fe oxide nanoparticles [Fig. 1(a)]. The synthesis and characterization of filled nanotubes are discussed in more detail by Tilmaciu *et al.* [20,21]. Transmission electron microscopy of hybrid nanotubes [Fig. 1(a)] reveals a discontinuous arrangement of crystallites, with lengths of a few tens of a nanometer, encapsulated inside the inner wall of the host DWCNT. The hybrid nanotubes are connected to Pd electrodes on top of an oxidized silicon substrate serving as a back gate, as shown in Fig. 1(b). The junctions are studied in a two-wire configuration, at very low temperature ($T = 40$ mK). Figure 1(c) shows a single trace of the differential conductance $G = dI/dV$ as a function of the gate voltage V_g. The differential conductance exhibits a series of peaks and dips, related to single-electron tunneling through discrete energy levels in the Coulomb blockade regime. The irregularity of the G amplitude modulation as a function of V_g emphasizes the presence of significant disorder, probably induced by the filling procedure.

We now consider quantum transport under the influence of a magnetic field B, applied in the plane of the junction and swept at a constant rate of 0.03 $\mathrm{T \cdot s^{-1}}$. Figure 2(a)

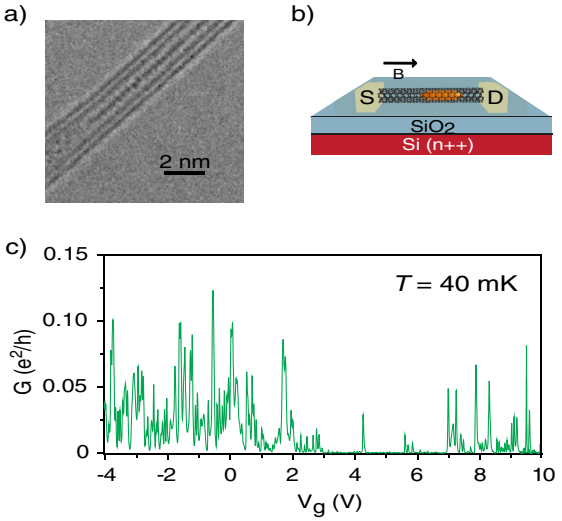

FIG. 1 (color online). (a) High resolution transmission electron microscope micrograph of a portion of an individual DWCNT, filled inside its inner shell with elongated nanoparticles. (b) Schematic representation of the device, consisting of a filled nanotube on top of an oxidized Si wafer (used as a back gate) and connected between source-drain electrodes (50 nm Pd). The typical junction length is 350 nm. Magnetic field is applied in plane and in the direction of the carbon nanotube. (c) Lock-in gate modulation of the device at 40 mK with zero source-drain bias ($V_{sd} = 0$).

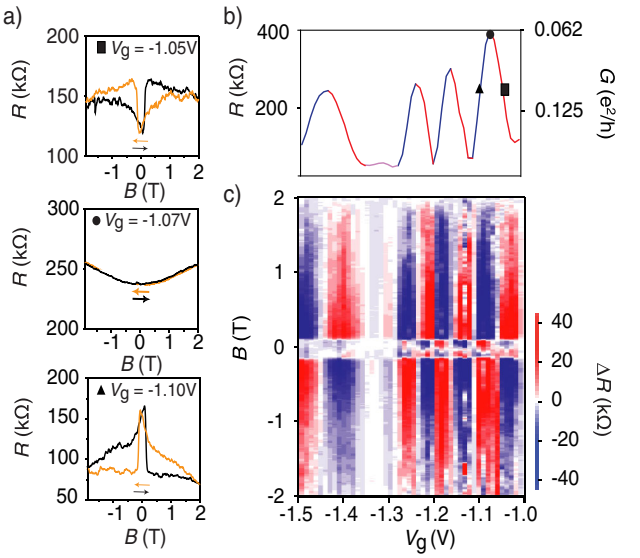

FIG. 2 (color online). Gate-dependent hysteresis of MR. (a) Plot of differential resistance R versus the magnetic field (B) from -1.8 to $+1.8$ T (back and forth) at different gate voltages. At $V_g = -1.05$ V, R jumps around $B = \pm 0.15$ T with a sharp increase in resistance. At $V_g = -1.07$ V, no hysteresis is observed. At $V_g = -1.10$ V, R jumps around $B = \pm 0.15$ T with a sharp drop in resistance. (b) Gate modulation of the differential resistance (R) in the gate voltage range $V_g = -1.5$ V to $V_g = -1$ V at $B = 0$ T. The color of the curve is related to the sign of its slope (red for positive and blue for negative). Indicated are the position of the gate voltages, where the plots of (a) were taken. (c) Hysteresis (ΔR) plot (difference between trace and retrace) in the same gate voltage region. Positive, negative, and zero hysteresis is color plotted as red, blue, and white, respectively. The sign of the hysteresis after the jump (positive magnetic field) and the slope of the gate modulation are correlated.

shows single traces of the differential resistance R resulting from B-field sweeps, at three different constant gate voltages V_g. For two of the three gate voltages shown in Fig. 2(a), hysteretic MR is observed. Abrupt resistance jumps of amplitude R_{sw} are detected symmetrically, for both sweeping field directions, at well-defined switching fields $B_{sw} = \pm 150$ mT. At $V_g = -1.05$ V, R increases from 120 to 165 kΩ and yields a positive MR of 37.5%. On the other hand, at $V_g = -1.10$ V, R decreases from 150 to 80 kΩ, after the jump occurred. This yields a negative MR of 53%. Furthermore, R_{sw} is suppressed at $V_g = -1.07$ V. We observe outstandingly high hysteretic MR features, the sign of which is gate tunable and which can even be turned off at specific gate voltages. Moreover, R is strongly hysteretic and relaxes as B is increased to larger values.

The gate-dependent hysteresis is investigated in more detail, for a large gate voltage range. Figure 2(c) shows the corresponding color-scale plot of the hysteretic part of the MR (the difference in R between the two sweep directions), as a function of B and V_g. The hysteresis color alternates red and blue as a function of V_g. This pattern corresponds to a series of positive and negative hysteretic MR features, separated by regions of completely suppressed MR [white regions in Fig. 2(c)]. The discontinuous jumps are observed at the same switching field B_{sw} and appear as two symmetric continuous lines, which remain independent of V_g. The well-defined value of B_{sw} for this V_g range is attributed to the magnetization reversal of a single encapsulated magnetic nanoparticle. Interestingly, the hysteretic MR is clearly correlated to the differential resistance of the device at zero field [Fig. 2(b)]. More precisely, the sign of R_{sw} alternates along with the sign of the differential resistance slope $\frac{dR}{dV_g}$ by sweeping V_g through Coulomb peaks. The hysteresis amplitude is strongly reduced when R depends weakly on V_g and is suppressed, in particular, at the maxima and minima of the R peaks. By studying the MR single traces directly as a function of V_g, a sudden gate shift can also be noticed at $B = B_{sw}$ [Fig. 3(a)]. The gate oscillations of R which occur when V_g is varied, for $B < B_{sw}$ and $B > B_{sw}$, are similar [Fig. 3(a)] though shifted by a finite amount $\Delta V_g \approx 5$ mV [Fig. 3(b)]. The shift is exactly the same in the case when the magnetic field sweep is retraced (not shown here). The influence of magnetization reversal at B_{sw} on the nanotube quantum dot is thus equivalent to a change in the offset charge.

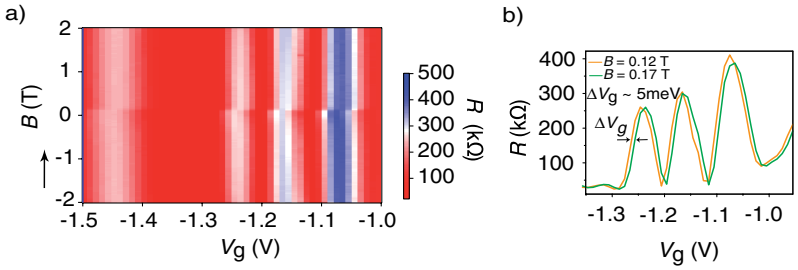

FIG. 3 (color online). Magnetization reversal induced shift of the Coulomb peaks. (a) R is color plotted for different V_g and B (traces from -2 to $+2$ T) in the same gate voltage region as in Fig. 2(b). (b) Horizontal cuts in (a) showing a right shift (ΔV_g) of 5 meV of the Coulomb oscillations after the switching field $B_{sw} = \pm 0.15$ T.

The gate-dependent hysteretic MR observed in our devices is attributed to a MCE, which is intimately correlated with charge transport in the Coulomb blockade regime. We now introduce a qualitative description of this effect and discuss its predominance in our devices. In the equivalent scheme in Fig. 4(a), the microscopic electronic coupling between the conductive DWCNT outer shell and the filling material is, to a first approximation, represented by an effective capacitance C_{eff}. The assumption that only the outer shell carries the current is supported by previous experimental and theoretical reports [22,23], suggesting a dramatic decrease in the inner shell conductivity due to significant filling-induced electron backscattering. This corroborates the fact that encapsulated magnetic objects are weakly coupled to charge transport in host DWCNTs.

We present here a phenomenological model based on the magneto-Coulomb effect, which can explain our results. Because of electronic coupling, the flow of electrons in the system is sensitive to the Zeeman energy of the nanoparticle $\Delta E_Z = -g\mu_B \mathbf{B}\cdot\mathbf{S}$, associated with its giant spin S in the B field, neglecting the magnetic anisotropy function. This energy corresponds to a potential energy variation in the nanometer-sized ferromagnet, as a function of the magnetic field, which can be expressed as the charging energy of an effective capacitance: $\Delta E_Z = \frac{\Delta Q^2}{2C_{\text{eff}}}$, where ΔQ is an effective charge held on C_{eff}, which accounts for the Zeeman effect. The electronic coupling between the outer carbon wall and the magnetic object is expected to be sufficiently strong for ΔQ to induce a significant gating effect on the nanotube. Moreover, the total energy of the nanoparticle is strongly dependent on the spin orientation, and the evolution of ΔQ reflects the spin reversal in the form of discontinuities in the amplitude ΔQ_{sw} at $B = \pm B_{sw}$, as shown in the diagram of Fig. 4(b). From the expressions for ΔQ and ΔE_Z, one obtains

$$\Delta Q_{sw} = \sqrt{2\alpha g \mu_B \mathrm{SB}_{sw}}, \tag{1}$$

where α is a constant including the cosine of the angle between the magnetic field and the easy axis of magnetization of the nanoparticle and the effective capacitive coupling factors relative to the conductive carbon shell and the nanoparticle environment. The induced effective charge variation, which is expected to be sharp at the instant of magnetization reversal of the nanoparticle, is equivalent to an effective gate voltage and should thus induce a resistance change ΔR [Fig. 4(b)], proportional to ΔQ:

$$\Delta R(B) = \frac{1}{C_g}\frac{dR}{dV_g}\Delta Q(B). \tag{2}$$

Equation (2) highlights the strong correlation of the MCE with the gate dependence of the resistance. The gate sensitive MR, shown in Figs. 2 and 3, shows the unambiguous signatures of a MCE. The general trend is in agreement with Eqs. (1) and (2), which account for both the amplitude and sign dependence of the MR's hysteresis

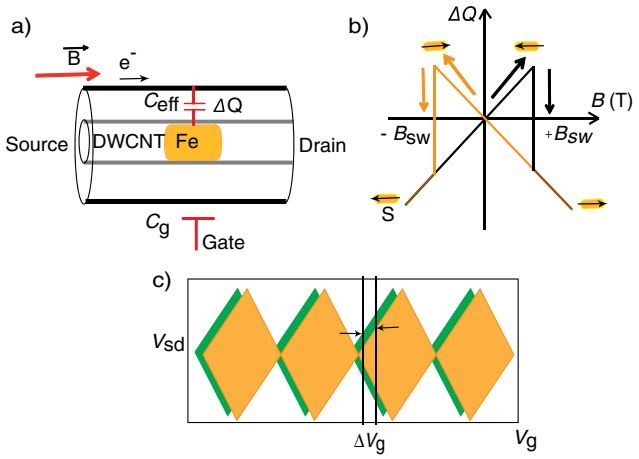

FIG. 4 (color online). Magneto-Coulomb effect. (a) Equivalent electrical circuit of the device. The nanoparticle is isolated from the environment because it is encapsulated inside the inner wall of a DWCNT. The outer wall is coupled to the gate electrode via the capacitance C_g. The effective coupling between the outer wall of the nanotube and the nanoparticles is shown as a capacitance C_{eff}. Only the outer wall conducts the current. (b) Schematic evolution of the effective charge ΔQ induced on the CNT by the Zeeman effect in the nanoparticle. ΔQ varies with applied magnetic field, until the nanoparticle switches its magnetization. At the switching field $B = \pm B_{sw}$, ΔQ changes discontinuously. (c) Shift of the Coulomb diamonds due to switching of the nanoparticles.

with V_g, as the nanotube quantum levels become resonant with the electrodes' Fermi level (Coulomb peaks). This MCE is very apparent at $B = \pm B_{sw}$, at which there is a sudden variation in the potential energy of the magnet accumulated by the Zeeman effect. This change can be translated into a variation of the chemical potential of nanotube by the capacitive coupling. This outcome highlights the gatelike effect of MCE, visible at $B = \pm B_{sw}$. This chemical potential variation of the nanotube corresponds to a finite shift of the discrete energy levels in the dot, with respect to the electrodes' Fermi energies [Fig. 4(c)]. The effective shift of the nanotube's energy levels due to the switching of nanoparticles is given by $\Delta\epsilon_{shift} \approx 0.1$ meV (with $\Delta V_g = 5$ meV [Fig. 3(b)]). The rate at which the voltage applied to the back gate changes the electrostatic potential of the dot is $C_g/C = 0.02$ (see [24]). The charging energy of the nanotube U_c is 1 meV, as deduced from the Coulomb blockade features of the device (see [24]). Indeed, though the coupling to the nanomagnet is not sufficient to change the charge state of the nanotube, the spin flip influence induces yet strong features on the electronic transport, providing a sensitive nanotube quantum dot detector.

Although it is not easy to estimate the effective coupling between the nanotube and the magnetic object it contains, some hints about the efficiency of the device can be inferred from simple energy scale considerations. Let us consider, for example, an iron nanoparticle of 100 spins ($S = 100$, which is a likely particle size considering the TEM images), with a switching field $B_{sw} = 0.15$ T. The Zeeman energy change resulting from the switching would be $\Delta E_Z = 10$ meV, which is much higher than the effective electrostatic energy shift ($\Delta\epsilon_{shift}$) we observed in the gate modulation of our device. The coupling turns out to be poorly efficient, but the use of a quantum dot as a sensor still allows the straightforward detection of such low energies.

In conclusion, we have measured a new gate-dependent MR, which differs from that described in previous reports in which the MCE originated from the contact between nanostructures and ferromagnetic leads. In our case, the sign of the magnetoresistance of carbon nanotube is completely tunable by gate voltage. The clear correlation between the slope of the gate modulation of the nanotube and the hysteresis due to switching of the magnetization is a unique feature we observed. Indeed, here the MCE is induced by taking advantage of the local coupling of a nanotube quantum dot with low-dimensional magnets and does not imply the existence of any ferromagnetic contact. This new effect could be generalized to different nanomagnets, by using DWCNTs filled with various materials, or even functionalized with molecules, in order to provide a powerful technique for reading the magnetic properties of single nanomagnets coupled to CNT transistors.

This work is partially supported by the ANR-PNANO project MolNanoSpin No. ANR-08-NANO-002, ERC Advanced Grant MolNanoSpin No. 226558, and STEP MolSpinQIP. S. D. acknowledges the financial support from the RTRA Nanosciences Foundation. Samples were fabricated in the NANOFAB facility of the Neel Institute. We thank F. Balestro, N. Bendiab, L. Bogani, E. Bonet, T. Crozes, E. Eyraud, R. Haettel, C. Hoarau, D. Lepoittevin, R. Maurand, M. Monthioux, V. Reita, and C. Thirion.

[1] P. Seneor, A. Bernand-Mantel, and F. Petroff, J. Phys. Condens. Matter **19**, 165222 (2007).
[2] A. R. Rocha *et al.*, Nature Mater. **4**, 335 (2005).
[3] L. Bogani and W. Wernsdorfer, Nature Mater. **7**, 179 (2008).
[4] R. Hanson, L. P. Kouwenhoven, J. R. Petta, S. Tarucha, and L. M. K. Vandersypen, Rev. Mod. Phys. **79**, 1217 (2007).
[5] S. D. Bader, Rev. Mod. Phys. **78**, 1 (2006).
[6] M. Urdampilleta *et al.*, Nature Mater. **10**, 502 (2011).
[7] K. Ono, H. Shimada, and Y. Ootuka, J. Phys. Soc. Jpn. **66**, 1261 (1997).
[8] H. Shimada, K. Ono, and Y. Ootuka, J. Phys. Soc. Jpn. **67**, 1359 (1998).
[9] J. Wunderlich *et al.*, Solid State Commun. **144**, 536 (2007).
[10] A. Bernand-Mantel *et al.*, Nature Phys. **5**, 920 (2009).
[11] A. Bernand-Mantel *et al.*, Appl. Phys. Lett. **89**, 062502 (2006).
[12] F. A. Zwanenburg, D. W. van der Mast, H. B. Heersche, E. P. A. Bakkers, and L. P. Kouwenhoven, Nano Lett. **9**, 2704 (2009).
[13] S. J. van der Molen, N. Tombros, and B. J. van Wees, Phys. Rev. B **73**, 220406(R) (2006).
[14] S. Sahoo *et al.*, Nature Phys. **1**, 99 (2005).
[15] K. Tsukagoshi, B. W. Alphenaar, and H. Ago, Nature (London) **401**, 572 (1999).
[16] H. T. Man, I. J. W. Wever, and A. F. Morpugo, Phys. Rev. B **73**, 241401(R) (2006).
[17] L. Bogani *et al.*, Angew. Chem., Int. Ed. **48**, 746 (2009).
[18] M. Monthioux, E. Flahaut, and J. P. Cleuziou, J. Mater. Res. **21**, 2774 (2006).
[19] J. P. Cleuziou *et al.*, ACS Nano **5**, 2348 (2011).
[20] E. Flahaut, R. Bacsa, A. Peigney, and C. Laurent, Chem. Commun. (Cambridge) 12 (**2003**) 1442.
[21] C. Tilmaciu *et al.*, Chem. Commun. (Cambridge) 43 (**2009**) 6664.
[22] X. Blase and E. R. Margine, Appl. Phys. Lett. **94**, 173103 (2009).
[23] J. A. Fürst, M. Brandbyge, A. P. Jauho, and K. Stokbro, Phys. Rev. B **78**, 195405 (2008).
[24] See Supplemental Material at http://link.aps.org/supplemental/10.1103/PhysRevLett.107.186804 for the stability diagram (Coulomb diamonds) of the device and the magnetization reversal of different nanoparticles inside the nanotube.